Stabilization of Grain Boundary Morphologies in Lamellar Block Copolymer/Nanoparticle Blends

Jessica Listak and Michael R. Bockstaller*

Department of Materials Science and Engineering, Carnegie Mellon University, 5000 Forbes Ave., Pittsburgh, Pennsylvania 15213

Received April 6, 2006; Revised Manuscript Received June 20, 2006

ABSTRACT: Polymer-coated nanoparticle additives are shown to stabilize the formation of high-energy tilt and twist grain boundary structures in amorphous lamellar block copolymer/nanoparticle blends. The distribution of the particle additives within the grain boundary region depends on the level of perturbation of the equilibrium structure and presents analogies to previously described block copolymer/homopolymer blends. At small tilt angles (chevron grain boundary) the particle distribution is equal to the equilibrium distribution (here: center location of PS-coated gold particles within the PS domains of a PS−PEP block copolymer) whereas at larger tilt angles (omega or T-junction grain boundary structure) the particles are found to selectively swell the high elastic energy regions along the grain boundary, thereby stabilizing the formation of otherwise energetically unfavorable grain boundary structures presumably through the relaxation of chains in the grain boundary region. The direct visualization of the swelling process provides the first experimental evidence for the mechanism of stabilization of energetically unfavorable grain boundary structures by selective swelling and stress relief that was previously postulated for block copolymer/homopolymer blends and presents a model system for comparison with theoretical predictions.

Introduction

Current interest in block copolymer/nanoparticle (BCP/NP) blends is driven by two major motivations: from a fundamental perspective, BCP/NP mixtures represent fascinating model systems to study the structure formation in soft/hard heterogeneous materials in which subtle changes of entropic or enthalpic interactions can result in different morphologies.[1−3] From a more application-oriented point of view, BCP/NP composite materials have been shown to exhibit intriguing optical and mechanical properties that arise from the control of nanoparticle location and—in the case of anisotropic particle additives—orientation within the copolymer matrix.[4] While the detailed implications of the particle and copolymer architecture for the composite's microstructure remain elusive, recent work has highlighted the relevance of the materials' characteristic length scales (i.e., the relative particle and copolymer domain size) as well as enthalpic interactions on the final equilibrium microstructure of enthalpic neutralized BCP/NP blends.[1−3,5,6] Enthalpic neutralization of the particle inclusions to one of the block copolymer domains, as will be relevant in this paper, is typically realized by modifying the particle's surface with a low molecular weight homopolymer that is a chemical analogue to one of the block copolymer domains.[7] Whereas the study of the equilibrium microstructure formation process contributes important insight into the physics of self-organization of heterogeneous materials, the ultimate properties of the nanocomposites on the macroscopic scale are intimately related to the defect and grain boundary structure of the material on the microscopic level. Gido and Thomas studied the grain boundary formation in amorphous lamellar block copolymer materials and identified—dependent on the deformation mechanism (twisting or bending) of an initially aligned lamellar bicrystal—twist (helicoid and Scherk surface) and tilt (chevron, omega and T-junction) grain boundary morphologies.[8] The deformation modes of a lamellar bicrystal giving rise to the various grain boundary structures are illustrated in Scheme 1. The occurrence of defects and grain boundaries is inherent in the self-organization of block copolymers and has been related to the nucleation and growth of ordered grains during the structure evolution process, the superposition of stress fields around disclinations, and mechanically induced kinking or buckling of domains, e.g., induced by inhomogeneous solvent evaporation during the late processing stages.[9,10] Assuming a fixed orientation of the lamellae during the nucleation state, it can be expected that the frequency of occurrence of a particular defect configuration will be proportional to the Boltzman factor involving the energy of the respective defect.[11] Recent numerical simulations by Duque et al. suggest that the formation of discontinuous tilt boundaries, i.e., T-junction grain boundaries, is particularly unfavorable energetically, and thus T-junctions are unlikely to occur in block copolymer microstructures.[12] Furthermore, in their paper the authors suggest that the free energy per unit surface area in T-junction boundaries is effectively lowered by blending the copolymer with a homopolymer that is chemically equal to one of the copolymer components and that facilitates partial relief of copolymer stretching in the grain boundary region. Recently, Burgaz et al. demonstrated the higher frequency of T-junction grain boundaries in blends of poly(styrene-*b*-isoprene) and poly(isoprene) and thus provided evidence supporting the prediction.[13] However, strict experimental proof of the role of the homopolymers in stabilizing the grain boundary structure has not yet been available due to the difficulty of identifying the homopolymer within the copolymer microstructure. This article presents first results on the stabilization of high angle tilt (symmetric and asymmetric) and twist grain boundary structures in amorphous lamellar block copolymer/particle composites and demonstrates the implications of the local disruption of the equilibrium microdomain structure for the particle distribution. Interestingly, the response of polymer-coated nanoparticle additives with an effective particle (i.e., particle core plus polymer shell) diameter much smaller than the characteristic copolymer domain size to

* Corresponding author: e-mail Bockstaller@cmu.edu; phone 412 268 2709; Fax 412 268 7247.

10.1021/ma060778q CCC: $33.50
Published on Web 08/01/2006

Scheme 1. Illustration of the Deformation Modes of a Lamellar Bicrystal Resulting in (a) Pure Tilt and (b) Pure Twist Grain Boundary Structures[a]

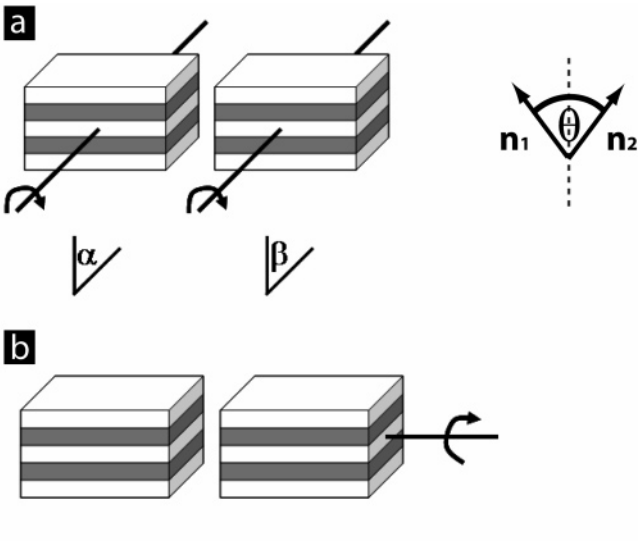

[a] The tilt angle θ is measured between the layer normals n_1 and n_2. Note that symmetric tilt grain boundary formation requires $\alpha = -\beta$ (with $|\alpha| + |\beta| = \theta$) as well as the grain boundary plane (dotted line) bisecting the tilt angle θ. See text for more details.

structural imperfections exhibits analogies to theoretical predictions for homopolymer additives. In particular, particle additives are found to selectively swell the high elastic energy regions along high angle tilt and twist grain boundaries and form dense aggregate-like structures that can easily be identified by electron microscopy. The results thus provide strong experimental support for the proposed mechanism of stabilization of grain boundary structures in block copolymer/homopolymer blends due to the selective swelling of high energy grain boundary regions and the associated relief of mechanical stress.

Experimental Section

Materials in our study consist of poly(styrene)-coated gold nanocrystals (AuSPS) and a near symmetric poly(styrene-*b*-ethylene propylene) (PS−PEP) block copolymer with a respective molecular weight of the constituting blocks of 45 and 47 kg/mol. The block copolymer in this study was donated by Kraton Polymers and was obtained by hydrogenation of the respective poly(styrene-*b*-isoprene) prepolymer. ^{1}H NMR studies revealed that the polymer contains about 1% of residual isoprene units. PS-coated gold nanocrystals with a mean core diameter of 3.5 nm were synthesized following the phase transfer approach developed by Brust et al.[14] The synthesis of thiol-terminated oligomeric styrene ligands with degree of polymerization $P \sim 10$ (equal to a molecular weight of $M_n = 1.04$ kg/mol) and a degree of polydispersity PD ~ 1.04 as well as details of particle purification and characterization has been described in ref 15. The grafting density of PS ligands on the particle surface was determined by TGA to be $\rho_{PS} \sim 0.02/\text{Å}^2$, somewhat lower than what was reported previously for short chain aliphatic ligands.[14] Block copolymer/nanocrystal composite films of about 1 mm thickness were obtained by film casting a 5% polymer solution in nonpreferential solvent (toluene) admixed with nanocrystals to result in a final amount of inorganic component in the composite of 1 vol %. The resulting films were subsequently annealed in saturated toluene atmosphere for 24 h at 60 °C before drying in a vacuum for 48 h. Films were microsectioned at −90 °C using a LEICA EM FCS cryo-ultramicrotome.

Transmission electron microscopy was performed using a JEOL 2000 FX electron microscope. Imaging was done by using amplitude and phase contrast. Where applicable (see Figures 3b,c and 4), specimens were stained using ruthenium tetroxide (obtained from EM Sciences) in order to enhance contrast by selective oxidation of the residual unsaturated groups in the PEP block.

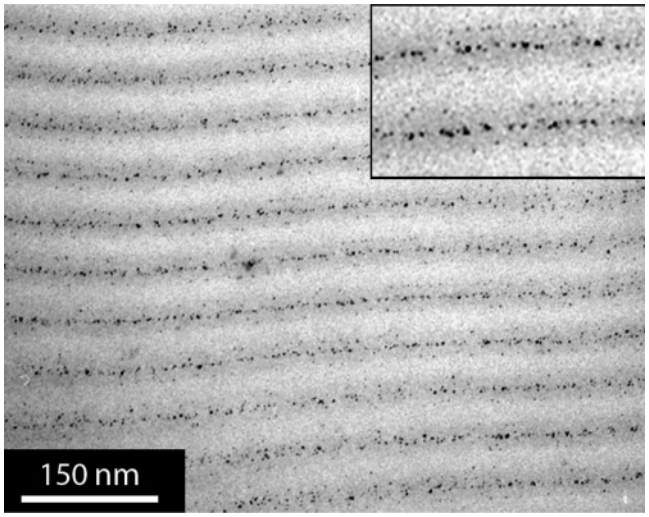

Figure 1. Electron micrograph of the unstained PS−PEP/AuSPS composite microstructure (see text). The micrograph reveals the lamellar equilibrium microdomain morphology with respective domain spacing of about 25 nm. PS-coated gold nanoparticles (dark dots, 3.5 nm core diameter) populate the center regions of the PS domains (darker domain). Inset shows a magnified area element.

Results and Discussion

Figure 1 shows a cross-sectional micrograph revealing the equilibrium microstructure of the PS−PEP/AuSPS composite: AuSPS nanocrystals preferentially sequester within the PS domain of the block copolymer and locate in the center region of the domains. The center distribution of the gold nanocrystals is in contrast to previous results that were obtained for very high molecular weight block copolymers of equal composition (800 kg/mol total molecular weight), in which AuSPS particles were observed to randomly distribute within the PS domain.[15,16] Given the very similar chemical composition in both cases we reason that the abundance of chain ends in the center region of the domain supports the accommodation of inclusions as the relative particle-to-domain size increases. We note that this observation supports previous studies on lamellar block copolymer/homopolymer blends which demonstrated both experimentally and theoretically that with increasing molecular weight, homopolymer additives will tend to concentrate within the center of the block copolymer domains[17,18] and is also in agreement with predictions of recent simulation studies on the structure formation in block copolymer/nanoparticle composites.[6] A large area view of the microstructure is depicted in Figure 2 that presents a low-magnification electron micrograph of the specimen. The micrograph clearly reveals various twist and tilt grain boundaries that separate the different grains of uniform respective lamellar orientation. By analysis of a series of micrographs such as the one shown in Figure 2, we estimate the average grain size in our sample to be about 42 μm^3.

Effect of Particle Additives on the Formation of Tilt Grain Boundary Structures. Tilt grain boundary structures involve a rotation between adjacent grains about an axis in the plane of the grain boundary, as illustrated in Scheme 1. A tilt grain boundary is called symmetric if the boundary plane bisects the angle of rotation between the two grains. Figure 3 depicts typical examples of the three tilt grain boundary structures that were observed in our samples: chevron-type (i.e., small tilt angle, symmetric deformation; Figure 3a), omega (i.e., large tilt angle, symmetric deformation; Figure 3b), and T-junction (i.e., about

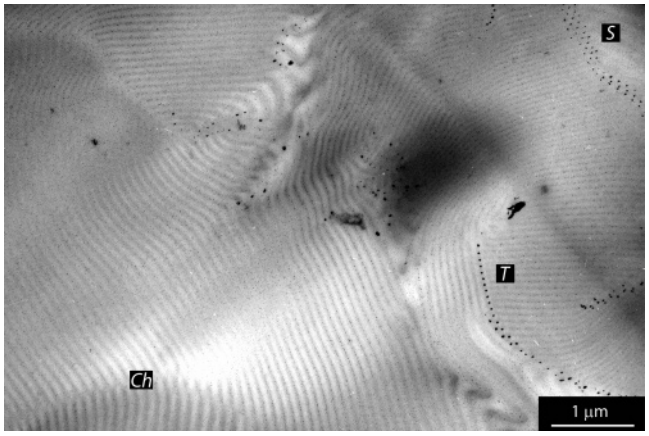

Figure 2. Low-magnification electron micrograph of the unstained composite microstructure. Several tilt and twist grain boundaries separating grains of distinct lamellae orientation can be identified. Abbreviations of pure tilt or twist grain boundary structures: Ch = chevron (tilt), T = T-junction (tilt), S = Scherk surface (twist). Gold particles swell the high-energy regions along the T-junction grain boundaries (dark dots). Note that at the given low magnification individual particles can hardly be resolved.

90° tilt angle, asymmetric deformation; Figure 3c). The figure reveals the formation of periodic particle aggregates across the omega and T-junction boundaries. The transition from the chevron to the omega grain boundary structure that accompanies the gradual increase in tilt angle between the lamellar grains is shown in Figure 4 (from the upper right to the lower left of the micrograph). The micrograph confirms that at low tilt angles (chevron) the particle distribution remains unaffected (no aggregate formation), whereas accumulation of particles within the grain boundary region is observed at larger tilt angles, about coinciding with the occurrence of the omega grain boundary structure. The driving force for the selective swelling of the grain boundary region will be discussed in more detail in the context of the stabilization of T-junction grain boundary structures where it will be argued that the accumulation of particles occurs in order to reduce energy penalties that are associated with the increasing distortion of the equilibrium microstructure. To perturb the equilibrium distribution of particles, the free energy penalty that is associated with the rearrangement of chains across the grain boundary must exceed the gain in free energy resulting from distributing the particles within the equilibrium positions (which is of the order of the thermal energy). It is thus natural to expect the existence of a threshold tilt angle in order to induce the accumulation of particles (for the present case the threshold tilt angle was determined to be $\theta_{crit} \approx 82°$ with θ denoting the angle between the layer normals, as illustrated in Scheme 1).

Figure 3c depicts a T-junction grain boundary structure that corresponds to a complete disruption of the continuous lamellar domain morphology. Because of the excessive chain stretching as well as increase in interfacial area, the T-junction grain boundary is particularly unfavorable energetically and has been predicted to occur only rarely in neat block copolymers.[12] The geometry of the T-junction grain boundary is illustrated in Scheme 2. Interestingly, we find about 15% of the tilt boundaries to be T-junction grain boundaries—a frequency that is comparable with results that were reported for block copolymer/homopolymer blends but which is about 1 order of magnitude higher than those that were observed in neat block copolymers of similar composition and sample preparation.[9,13] Remarkably, the AuSPS particles form discrete and regularly spaced aggregate structures of about equal size along the grain boundary

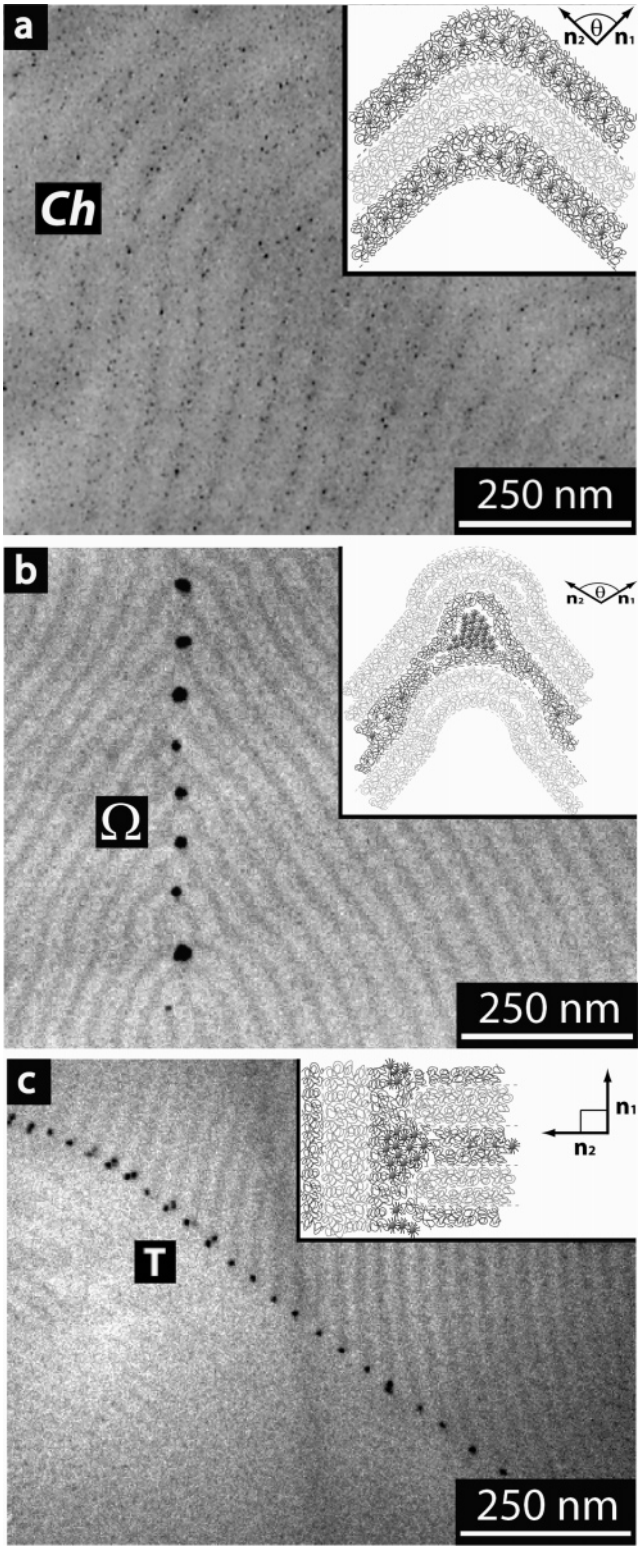

Figure 3. (a) Electron micrograph of the unstained PS−PEP/AuSPS depicting a chevron grain boundary structure ($\theta \approx 30°$). Particles are distributed similar to the equilibrium distribution shown in Figure 1 (a small tilt in the orientation of the specimen distorts the impression of particle alignment). (b) Electron micrograph of the stained PS−PEP/AuSPS depicting an omega-type grain boundary (Ω). The periodic array of aggregates reveals that particle accumulation occurs in high-energy regions across the boundary. (c) Electron micrograph of the stained PS−PEP/AuSPS depicting a T-junction grain boundary. The periodic array of aggregates reveals that particle accumulation occurs within the high-energy T-junctions across the boundary. Note that in the micrographs shown in (b) and (c) the PEP domains appear dark due to staining of residual isoprene units (see text). Insets of panels a−c illustrate the particle distribution within the boundary region.

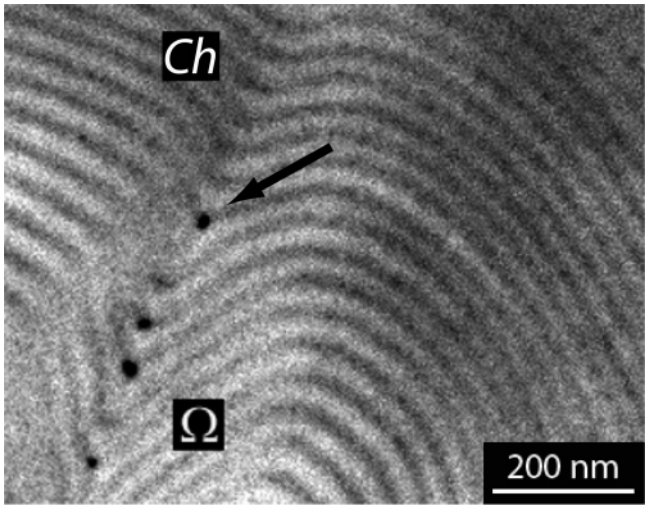

Figure 4. Electron micrograph of the stained PS−PEP/AuSPS depicting a gradual transition from low tilt angle chevron-type grain boundary structure (Ch) to high tilt angle omega-type grain boundary (Ω). Particle accumulation is observed above a threshold tilt angle of about $\theta_{crit} \approx 82°$ (threshold position indicated by arrow).

Scheme 2. Illustration of T-Junction Grain Boundary Geometry[a]

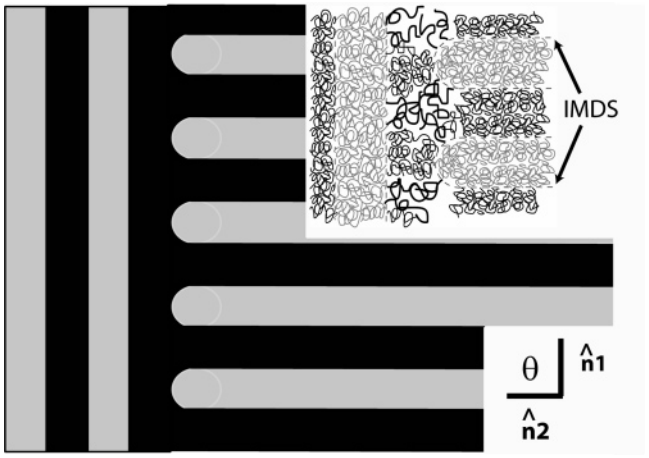

[a] Pure T-geometry requires $\theta = 90°$ (measured between the layer normals n_1 and n_2). Only one domain is continuous along the grain boundary whereas the other (the local minority domain) is disrupted and forms semicylindrical caps that terminate in the local majority domain. The inset illustrates the associated chain stretching (bold chains) of the local majority domain within the T-junction regions that arises due to the space-filling constraint. IMDS denotes the intermaterial dividing surface that separates adjacent domains.

(note that because of the low magnification and the staining individual particles cannot be resolved in Figure 3c). The spacing between the particle aggregates across the grain boundary is found to be close to the characteristic lamellar spacing of the microstructure. The regular arrangement of the aggregates within the structure—as is also observed in the case of the omega grain boundary structure—indicates that the accumulation of particles occurs during the film formation or annealing process in response to existing grain boundaries rather than the accidental alignment of several preformed aggregates inducing defect formation within the microstructure. Insight into the origin of aggregate formation and the nature of the stabilization of the grain boundary configuration is obtained from analysis of Figure 5a which depicts a higher magnification micrograph of a T-junction grain boundary (unstained specimen). The micrograph reveals that PEP semicylinders (brighter domain) constitute the local minority domain that terminates

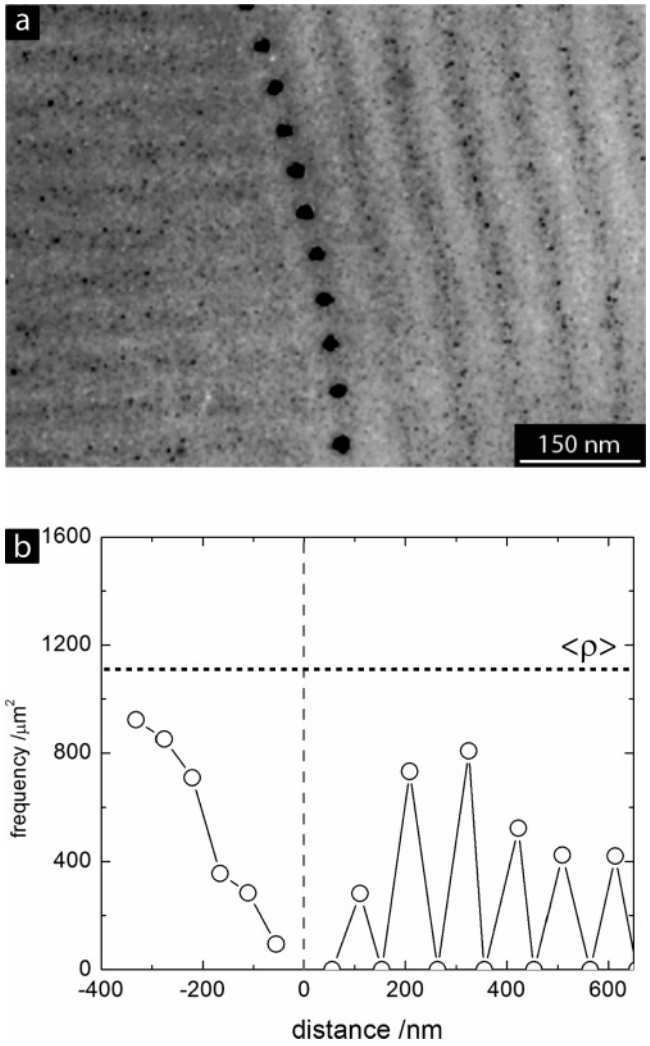

Figure 5. (a) Electron micrograph of the unstained PS−PEP/AuSPS depicting a magnified cross section of an individual T-junction grain boundary. PS constitutes local majority domains, PEP constitutes semicylindrical end-cap regions (local minority domain). Large dark dots along the grain boundary are the particle aggregates that form due to accumulation that is driven by the associated stress relief in the high-energy T-junction regions along the grain boundary (see text). Small dark dots are individual particles. (b) Particle frequency as a function of the distance and direction from the grain boundary (shown in panel a) calculated by particle counting across rectangular area elements of width $\Delta d = 50$ nm parallel to the boundary. The line joining the particle center positions along the grain boundary defines "zero" particle distance. $\langle\rho\rangle = (1/N)\Sigma_i(dn_i/da_i)$ denotes the equilibrium particle density with dn_i denoting the number of particles in area section da_i and N the total number of area sections (see text).

in the PS matrix that forms the continuous T-junction (local majority domain). This is in support of numerical simulations of the structure formation in block copolymer/homopolymer blends that predict the homopolymer−analogue copolymer domain to form the local majority domain along the grain boundary.[12] AuSPS particles are found to selectively swell the T-junction regions within the PS domains, as indicated in the inset of Figure 3c. This can be rationalized using a simple geometric argument. The formation of semicylindrical end-cap regions in the T-junction grain boundary structure increases the mean curvature of the intermaterial dividing surface (IMDS) and results in both increased interfacial area and chain stretching of the local "majority" domain (PS) in order to effectively fill space.[19] This situation is schematically depicted in the inset of Scheme 2. Selective swelling of these regions relaxes the mechanical stresses that are associated with the increase of chain

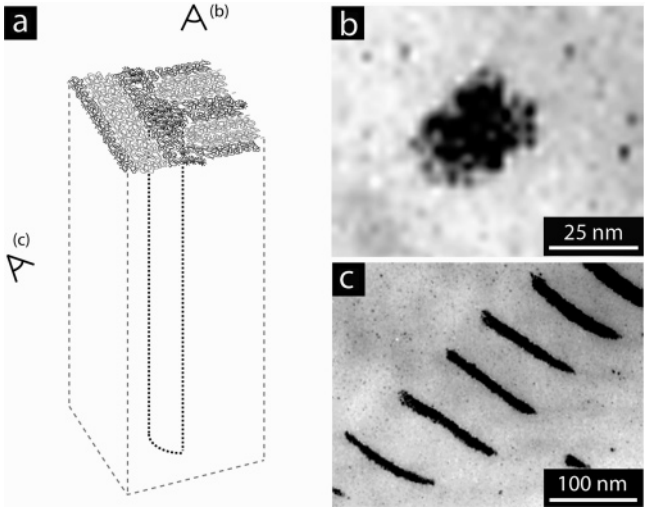

Figure 6. (a) Illustration of the 3D geometry of a T-junction grain boundary. Particles form stringlike aggregates along the grain boundary surface. (b) Cross-sectional view of a particle aggregate sectioned normal to the grain boundary surface. (c) Cross-sectional view of particle aggregates sectioned in off-normal direction to the boundary.

stretching and thus stabilizes the grain boundary. As a consequence, 3D "stringlike" particle aggregates form within the high-energy regions parallel to the grain boundary surface, and the micrographs depict a cross-sectional projection after sectioning normal to the string direction. Because of the periodicity of the microstructure, these aggregates are expected to be of equal size as is confirmed by the micrographs. The 3D nature of the aggregates is illustrated in Figure 6 where micrographs corresponding to normal and oblique sectioning direction are shown. Note that the observation of selective swelling of high-energy regions within the microstructure bears analogy to the mechanism of stabilization of T-junction grain boundary structures in block copolymer/homopolymer blends that was inferred from molecular level simulations and indirect experimental evidence.[12,13] The similarities in structure-formation characteristics between additives of very different architecture suggest that a unified prediction of the structure formation process in heterogeneous block copolymer blends should be feasible on the basis of universal descriptors (such as the total excluded volume) of the additive component. This will be explored in a forthcoming publication.

Careful observation of the particle distribution depicted in Figure 5a furthermore reveals that the nonuniform energy landscape associated with the formation of grain boundaries results in alterations of the particle distribution around the grain boundary. Figure 5b presents the particle frequency as a function of the distance and direction with respect to the grain boundary with distance $d = 0$ indicating the axis connecting the center positions of aggregates along the T-junction. Particle frequencies were calculated by superimposing a grid of rectangular area elements of $\Delta d = 50$ nm width, parallel to the grain boundary. On both sides of the grain boundary the particle density is found to decrease around the aggregate location and to increase to higher values (corresponding to about 75% of the equilibrium particle density) with increasing distance from the T-junction.[20] This suggests that the higher energy regions that are comprised of the stretched chains represent a potential well for the diffusing particles during the film formation or annealing process that consequently results in particle accumulation. The occurrence of particle depletion on both sides of the grain boundary implies that particles partially traverse the unfavorable PEP domain which is adjacent to the grain boundary during the annealing process. This can be interpreted as a consequence of the solvent annealing procedure. Since toluene is a good solvent for both particles and block copolymer, it effectively screens the interaction between the particles and the respective blocks, thus promoting the diffusion of particles even through the unfavorable polymer domain.[21] On the basis of this interpretation, the final concentration of T-junctions within the microstructure will depend on the subtle interplay between initial defect concentration after casting as well as the characteristic time scales for domain reorientation and particle diffusion during the annealing process. We note that the nonuniform particle distribution around the grain boundary indicates that the system is not in global equilibrium since—as the high-energy regions fill with particles and the associated potential energy gradient driving the accumulation process diminishes—complete homogenization of the particle density would be expected in the final equilibrium state. A more detailed analysis of the long-time annealing behavior will be necessary to gain insight into the final equilibrium morphology.

Effect of Particle Additives on the Formation of Twist Grain Boundary Structures. While the focus of the present paper is on the stabilization of high-energy tilt grain boundary structures, similar observations can be made for high-energy twist grain boundaries. Twist boundaries involve a rotation between adjacent grains about an axis normal the plane of the boundary, as illustrated in Scheme 1. Depending on the degree of twist, two grain boundary structures can be distinguished: the helicoid section at small twist angle and the Scherk boundary at large twist angles, respectively. For the purpose of the present paper the Scherk grain boundary structure is of particular interest because it has been proposed as a model for 90° twist boundaries in lamellar systems.[22,23] The Scherk surface is generated by smoothly joining two sets of planes that are aligned normal with respect to each other and has been extensively described in previous studies of grain boundary formation in block copolymer materials.[8,9] The geometry of the Scherk surface grain boundary structure is illustrated in Scheme 3. Using a self-consistent-field approach, Gido et al. demonstrated that the free energy density maximum occurs at the center of the saddles (close to the saddle point) across the grain boundary, where the stretching of chains is most unfavorable.[24] Figure 7 depicts the particle distribution about a Scherk-surface twist grain boundary (estimated twist angle is 80°), revealing the accumulation of particles within a regular array structure. A magnified view revealing the composition of the particle aggregates is shown in the inset of Figure 7. On the basis of the distance of the individual aggregates along the boundary that equals about the characteristic lamellar spacing of the block copolymer, we reason that particle accumulation indeed occurs within the PS domains close to the saddle points of the Scherk surface, resulting in "checkerboard-like" particle arrays as illustrated in Scheme 3c. However, this conclusion is preliminary due to the limited number of twist grain boundary structures that were observed in the current study.

Conclusions

Understanding of the consequences of material characteristics and processing conditions on the equilibrium and grain boundary morphologies in block copolymer/nanoparticle blends will be essential for the development of applications that capitalize on the particular microstructure of the nanocomposite materials. The results presented in this paper suggest a close analogy between the mechanisms of grain boundary stabilization in block copolymers blended with small, polymer-functionalized nanoparticle or homopolymer additives. The direct visualization of

Scheme 3. Illustration of a 90° Scherk Surface Twist Grain Boundary Structure[a]

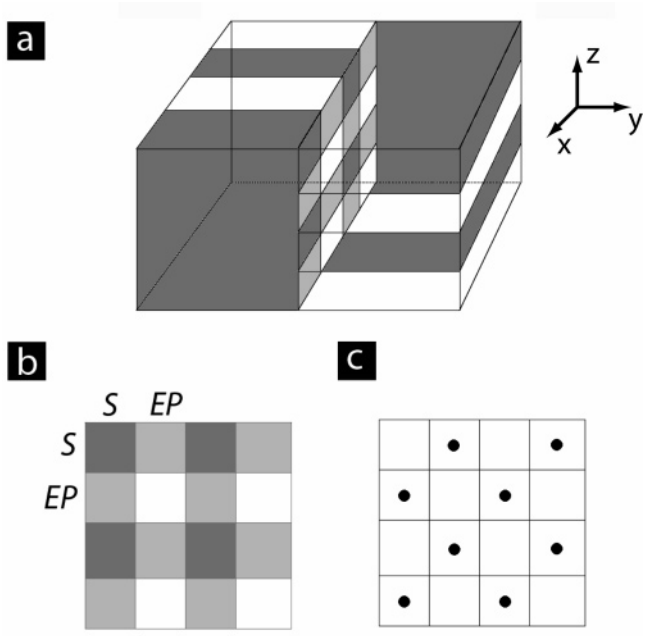

[a] Panel a: Perspective view of two lamellar grains twisted at 90° with respect to each other and forming the grain boundary. Panel b: projection of the grain boundary along *y*-axis direction. Dark gray and white square elements indicate where adjacent domains of PS ("S") and PEP ("EP") match up. Light gray area elements indicate the location of saddle surfaces. Panel c: dark dots represent the location of aggregates that form close to the saddle points across the grain boundary.

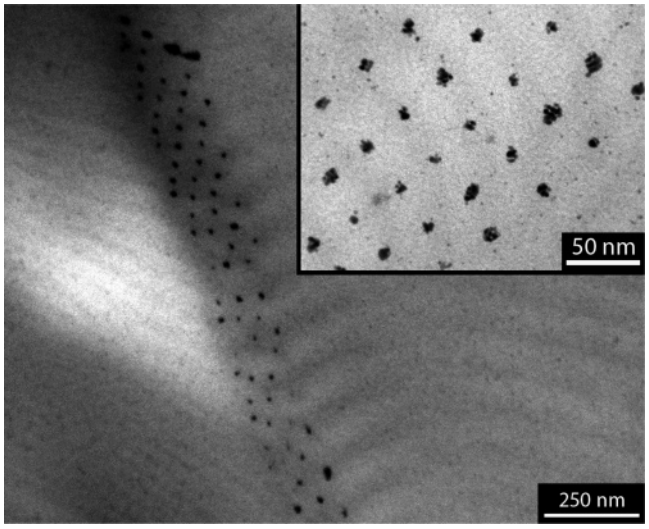

Figure 7. Electron micrograph of the unstained PS−PEP/AuSPS depicting a first Scherk surface twist grain boundary structure corresponding to a twist angle of about 80°. Particles accumulate within the high-energy regions close to the saddle points of the boundary surface (see text). Inset shows higher magnification of the regular array of particle aggregates formed along the grain boundary.

the swelling of regions of high elastic energy with nanoparticles provides the first direct experimental evidence for the mechanism of stabilization of energetically unfavorable grain boundary structures that was previously proposed for block copolymer/homopolymer blends and presents a model system for comparison with theoretical predictions. Even though the present study was focused on the characteristics of bulk composite materials, the major conclusions should also be applicable to the study of thin film morphologies. For example, recent simulations of the effect of homopolymer additives on the assembly of block copolymer thin films on prepatterned substrates with purposefully introduced defects predict stress relief to cause the concentration of homopolymer to increase in the defect region very similar to our observation.[25] One could envision that the replacement of one of the homopolymer additives by suitably modified particle additives will provide new opportunities to nanopattern surfaces.

Acknowledgment. Funding was provided by the Department of Materials Science and Engineering at Carnegie Mellon University and the Berkman Faculty Development Fund. J.L. acknowledges USX fellowship support by US Steel. The authors thank Kraton Polymers for the donation of polymer samples.

References and Notes

(1) Bockstaller, M. R.; Lapetnikov, Y.; Margel, S.; Thomas, E. L. *J. Am. Chem. Soc.* **2003**, *125*, 5276.
(2) Chiu, J. J.; Kim, B. J.; Kramer, E. J.; Pine, D. J. *J. Am. Chem. Soc.* **2005**, *127*, 5036.
(3) Jeng, U. S.; Sun, Y. S.; Lee, H. J.; Hsu, C. H.; Liang, K. S.; Yeh, S. W.; Wei, K. H. *Macromolecules* **2004**, *37*, 4617.
(4) Bockstaller, M. R.; Mickiewicz, R. A.; Thomas, E. L. *Adv. Mater.* **2005**, *17*, 1331. Park, C.; Yoon, J.; Thomas, E. L. *Polymer* **2003**, *44*, 6725. Yeh, S. W.; Wu, T. L.; Wei, K. H. *Nanotechnology* **2005**, *16*, 683. Bockstaller, M. R.; Thomas, E. L. *Phys. Rev. Lett.* **2004**, *93*, 166106.
(5) Kim, B. J.; Chiu, J. J.; Yi, G. R.; Pine, D. J.; Kramer, E. J. *Adv. Mater.* **2005**, *17*, 2618.
(6) Thompson, R. B.; Ginzburg, V. V.; Matsen, M. W.; Balazs, A. C. *Science* **2001**, *292*, 2469. Lee, J. Y.; Thompson, R. B.; Jasnow, D.; Balazs, A. C. *Macromolecules* **2002**, *35*, 4855.
(7) The assumption of enthalpic neutralization, i.e., a Flory interaction parameter $\chi_{PA} = 0$ between a polymer-coated particle "P" and the polymer matrix "A", strictly speaking does not apply to a system in which the polymer grafted to the particles' surface and the matrix polymer are chemically identical. Similar to star-polymer/homopolymer blends, the interaction parameter should be viewed as being "effective" and constituted by an entropic and enthalpic part. The entropic loss that is associated with the connectivity of the "star particle" will contribute a repulsive component to the overall interaction and render χ_{PA} positive (e.g. see: Fredrickson, G. H.; Liu, A.; Bates, F. S. *Macromolecules* **1994**, *27*, 2503; Lee, J. S.; Quirk, R. P.; Foster, M. D. *Macromolecules* **2004**, *37*, 10199).
(8) Gido, S. P.; Gunther, J.; Thomas, E. L.; Hoffman, D. *Macromolecules* **1993**, *26*, 4506.
(9) Gido, S. P.; Thomas, E. L. *Macromolecules* **1994**, *27*, 6137.
(10) Fredrickson, G. H.; Binder, K. *J. Chem. Phys.* **1989**, *91*, 7265.
(11) Tsori, Y.; Andelman, D.; Schick, M. *Phys. Rev. E* **2000**, *61*, 2848.
(12) Duque, D.; Katsov, K.; Schick, M. *J. Chem. Phys.* **2002**, *117*, 10315.
(13) Burgaz, E.; Gido, S. P. *Macromolecules* **2000**, *33*, 8739.
(14) Brust, M.; Bethell, M. W. D.; Schiffrin, D. J.; Whyman, R. *J. Chem. Soc., Chem. Commun.* **1994**, 801.
(15) Bockstaller, M.; Kolb, R.; Thomas, E. L. *Adv. Mater.* **2001**, *13*, 1786.
(16) Bockstaller, M. R.; Thomas, E. L. *J. Phys. Chem. B* **2003**, *107*, 10017.
(17) Hashimoto, T.; Tanaka, H.; Hasegawa, H. *Macromolecules* **1990**, *23*, 4378. Winey, K.; Fetters, L.; Thomas, E. L. *Macromolecules* **1991**, *24*, 6182.
(18) Shull, K. R.; Winey, K. *Macromolecules* **1992**, *25*, 2637.
(19) Wang, Z. G.; Safran, S. A. *J. Chem. Phys.* **1991**, *94*, 679.
(20) The equilibrium particle density $\langle\rho\rangle = (1/N)\Sigma_i(dn_i/da_i)$, where dn_i denotes the number of particles in area section da_i and N the total number of area sections, was determined by particle counting in defect-free regions of the microstructure (i.e., by analysis of micrographs such as Figure 1). Note that in Figure 5b the particle density in the negative-*x* direction levels off at values close to the equilibrium particle density at distances of about 400 nm from the junction. A qualitatively similar behavior is found in the positive-*x* direction, however, with some discrepancy that is attributed to insufficient area sampling.
(21) Kent, M.; Tirrell, M.; Lodge, T. P. *Macromolecules* **1992**, *25*, 5383.
(22) Helfand, E.; Wasserman, Z. R. *Macromolecules* **1976**, *9*, 879.
(23) Thomas, E. L.; Anderson, D. M.; Henkee, C. S.; Hoffman, D. *Nature (London)* **1988**, *334*, 598.
(24) Gido, S. P.; Thomas, E. L. *Macromolecules* **1994**, *27*, 849.
(25) Stoykovich, M. P.; Müller, M.; Kim, S. O.; Solak, H. H.; Edwards, E. W.; de Pablo, J. J.; Nealey, P. F. *Science* **2005**, *308*, 1442.

MA060778Q